Phys Chem Minerals (2003) 30: 321–329
DOI 10.1007/s00269-003-0328-0

ORIGINAL PAPER

S. D. Jacobsen · J. R. Smyth · R. J. Swope

Thermal expansion of hydrated six-coordinate silicon in thaumasite, $Ca_3Si(OH)_6(CO_3)(SO_4)\cdot 12H_2O$

Received: 3 June 2002 / Accepted: 28 September 2002

Abstract Thaumasite, $Ca_3Si(OH)_6(CO_3)(SO_4)12H_2O$, occurs as a low-temperature secondary alteration phase in mafic igneous and metamorphic rocks, and is recognized as a product and indicator of sulfate attack in Portland cement. It is also the only mineral known to contain silicon in six-coordination with hydroxyl $(OH)^-$ that is stable at ambient P–T conditions. Thermal expansion of the various components of this unusual structure has been determined from single-crystal X-ray structure refinements of natural thaumasite at 130 and 298 K. No phase transitions were observed over this temperature range. Cell parameters at room temperature are: $a = 11.0538(6)$ Å, $c = 10.4111(8)$ Å and $V = 1101.67(10)$ Å^3, and were measured at intervals of about 50 K between 130 and 298 K, resulting in mean axial and volumetric coefficients of thermal expansion ($\times 10^{-5}$K^{-1}); $\alpha_a = 1.7(1)$, $\alpha_c = 2.1(2)$, and $\alpha_V = 5.6(2)$. Although the unit cell and $^{VIII}CaO_8$ polyhedra show significant positive thermal expansion over this temperature range, the silicate octahedron, sulfate tetrahedron, and carbonate group show zero or negative thermal expansion, with $\alpha_V(^{VI}SiO_6) = -0.6 \pm 1.1$, $\alpha_V(^{IV}SO_4) = -5.8 \pm 1.4$, and $\alpha_R(C\text{–}O) = 0.0 \pm 1.8$ ($\times 10^{-5}$ K^{-1}). Most of the thermal expansion is accommodated by lengthening of the R(O...O) hydrogen bond distances by on average 5σ, although the hydrogen bonds involving hydroxyl sites on ^{VI}Si expand twice as much as those on molecular water, causing the $[Ca_3Si(OH)_6(H_2O)_{12}]^{4+}$ columns to expand in diameter more than they move apart over this temperature range. The average Si–OH bond length of the six-coordinated Si atom $\langle R(^{VI}Si\text{–}OH)\rangle$ in thaumasite is 1.783(1) Å, being about 0.02 Å ($\sim 20\sigma$) shorter than ^{VI}Si–OH in the dense hydrous magnesium silicate, phase D, $MgSi_2H_2O_6$.

Keywords Si–OH · Octahedrally coordinated silicon · Hydrogen bonding · Thermal expansion · Thaumasite

S. D. Jacobsen (✉) · J. R. Smyth
Department of Geological Sciences,
University of Colorado, Boulder,
Colarado 80309 USA

R. J. Swope
Department of Geology,
Indiana University-Purdue University,
Indianapolis, Indiana 46202 USA

Present address: S. D. Jacobsen
Bayerisches Geoinstitut
Universität Bayreuth
95440 Bayreuth, Germany
Tel.: +49 921 553739
Fax: +49 921 553769
e-mail: Steven.Jacobsen@uni-bayreuth.de

Introduction

The silicate minerals that make up most of Earth's crust nearly always contain Si in four-coordination with oxygen. Si–O bonds on ^{IV}Si are rather short and have high Pauling bond strengths, with an average bond distance $\langle R\,(^{IV}Si\text{–}O)\rangle$ of about 1.626 Å for natural silicate minerals (Pauling 1980; Gibbs 1982). The silicate tetrahedron is an exceptionally incompressible structural unit with a bulk modulus usually greater than 400 GPa (e.g., Smyth et al. 2001) and typically exhibits zero thermal expansion below 1200 K (Downs et al. 1992). At pressures above 10 GPa, silicon atoms can achieve six-coordination with oxygen atoms resulting in the $(SiO_6)^{8-}$ octahedron, having longer Si–O bonds with $\langle R(^{VI}Si\text{–}O)\rangle$ of about 1.794 Å, but an overall reduction in molar volume, usually being accommodated by shortened O–O distances (Prewitt and Downs, 1998; Finger and Hazen 2001). High-pressure phases containing ^{VI}Si–O relevant to Earth's interior include stishovite–SiO_2 (Ross et al. 1990), and polymorphs of $MgSiO_3$ with the ilmenite (Horiuchi et al. 1982), majorite–garnet (Angel et al. 1989), and orthorhombic perovskite (Horiuchi et al. 1987) structures.

Hydration of silicate minerals normally occurs by protonation of oxygen positions that are not also bonded to silicon as in micas, amphiboles, and humites, or by incorporation of water molecules as in lawsonite and the zeolites. Silicate-oxygen sites have relatively deep electrostatic potentials and can become overbonded if

they are also protonated (Smyth 1989). For longer Si–O bonds, or silicate oxygens with more shallow electrostatic potentials, Si–OH becomes a potential hydration mechanism. The resulting bond is on average longer than Si–O, with $\langle R(^{IV}Si–OH)\rangle = 1.643$ Å, reported from the average of 31 known minerals and organic compounds containing 46 different ^{IV}Si–OH bonds with varying degrees of tetrahedral polymerization (Nyfeler and Armbruster 1998). Recently, we explored the crystal chemistry of a stoichiometrically hydrated silicate tetrahedron [$^{IV}SiO_3(OH)$] in the pyroxenoid serandite, $NaMn_2[Si_3O_8(OH)]$, and found $R(^{IV}Si–OH) = 1.628(1)$ Å, being consistent for ^{IV}Si–OH having two bridging oxygens, and is associated with one of the strongest hydrogen bonds known in minerals with $R(O...O) = 2.464(1)$ Å (Jacobsen et al. 2000). Here, we investigate the crystal chemistry and thermal expansion of the hydrated silicate octahedron [$^{VI}Si(OH)_6$] in the naturally occurring mineral thaumasite, $Ca_3Si(OH)_6(CO_3)(SO_4)12H_2O$, from new single-crystal X-ray structure refinements at 130 and 298 K.

Thaumasite is the only mineral known to contain silicon in six-coordination with hydroxyl that is stable at (or near) ambient pressures and temperatures. The only other fully hydrated silica octahedron is found in the synthetic high-pressure dense magnesium silicate, phase D, $MgSi_2H_2O_6$ (Yang et al. 1997; Frost and Fei 1998). Thaumasite therefore affords us the unique opportunity to study the effect of hydration on six-coordinate silicon in a mineral within its stability field. Thaumasite begins to dehydrate at temperatures of about 380 K (Brough and Atkinson 2001), so we have chosen to study thermal expansion of thaumasite between 130 and 300 K. The cryogenic temperatures offer reduced thermal vibrations, facilitating location of hydrogen positions at non-ambient temperatures (four water and two hydroxyl groups). Structure refinements below room temperature also mimic the effect of slightly increasing pressure due to the inverse relationship between increasing temperature and increasing pressure (e.g., Hazen et al. 2001). Further, the behavior of thaumasite at lower temperatures is useful in the context of thaumasite synthesis because lower temperatures (~273 K) appear to favor rapid crystal growth and may explain how Si achieves the six-coordination at room pressure (Aguilera et al. 2001). Sulfate attack of Portland cement by thaumasite is greatly accelerated at subzero temperatures, as evidenced from rapid deterioration of reinforced concrete foundations in the Arctic within just 2 years of construction (Bickley 1999).

Background and objectives

Thaumasite, $Ca_3Si(OH)_6(CO_3)(SO_4)12H_2O$ is hexagonal ($P6_3$) with $a \sim 11.03$ Å and $c \sim 10.40$ Å (e.g., Edge and Taylor 1971; Effenberger et al. 1983). It is over 50% water and hydroxyl by weight, with a correspondingly low density about twice that of ice, with $\rho_{calc} = 1.88$ g cm^{-3}. Moenke (1964) recognized that thaumasite probably contained octahedral silicon from infrared spectra, noting that several absorption bands below 1000 wavenumbers were similar to those observed in stishovite. Silicon-29 NMR spectroscopy confirms that Si is exclusively six-coordinate, with a measured chemical shift at −180 ppm (relative to TMS) in both natural and synthetic samples (Grimmer et al. 1980; Stebbins and Kanzaki 1991). Brough and Atkinson (2001) showed that micro-Raman spectroscopy can be used to identify thaumasite in high concentrations (and distinguish it from ettringite) using the ν_1 band assigned to ^{VI}Si at 658 cm^{-1}. A method of thaumasite synthesis is given by Aguilera et al. (2001).

Thaumasite is a member of the ettringite group of hydrated calcium sulfates that also includes ettringite, $Ca_6[Al(OH)_6]_2(SO_4)_3 \cdot 26H_2O$ (Moore and Taylor 1970), bentorite, $Ca_6[(Cr,Al)(OH)_6]_2(SO_4)_3 \cdot 26H_2O$; charlesite, $Ca_6[Al(OH)_6]_2(SO_4)_2B(OH)_4 \cdot 26H_2O$; sturmanite, $Ca_6[(Fe)(OH)_6]_2(SO_4)_{2.4}[B(OH)_4]_{1.2} \cdot 25H_2O$; jouravskite, Ca_3 [(Mn)$(OH)_6$] $(SO_4)(CO_3) \cdot 12H_2O$; and also most recently described, micheelsenite, $(Ca,Y)_3Al(PO_3OH,CO_3)(CO_3)(OH)_6 \cdot 12H_2O$ (McDonald et al. 2001). Barnett et al. (2000) showed that there is indeed a solid solution between thaumasite and ettringite (space group $P31c$) with double the c-axis of thaumasite. Between thaumasite and ettringite there is a short discontinuity in the a-axis dimension between 11.11 and 11.17 Å, most likely corresponding to a small immiscibility at the change in space group (Barnett et al. 2000). The crystal structure of thaumasite was determined by Edge and Taylor (1969, 1971), confirming the presence of ^{VI}Si–OH. The structure was refined by Zemann and Zobetz (1981) and Effenberger et al. (1983), although there are some important and substantial differences in the various refinements, particularly in the ^{VI}Si–OH bond lengths and deviations of the carbonate group from planarity.

Portland cement is a dehydrated mixture of Ca, Si, and Al oxides with or without added gypsum or calcite. When mixed with water at high pH, secondary mineralization can occur as precipitate from the initial gel. Thaumasite and ettringite are commonly formed in the porous matrix of aging cement, particularly in cold, moist environments where there is contact with sulfate-rich soils or fluids (Crammond 1985), and especially when limestone is used as a filling material (Hartshorn et al. 1999). The presence of thaumasite and ettringite in cement is known as sulfate attack and they are precursors to softening and even disintegration of the cement matrix (e.g., Hartshorn et al. 1999; Bensted 1999; Hobbs and Taylor 2000; Santhanam et al. 2001). These studies and others have reported significant deterioration of concrete structures below ground in motorway bridges and other structures, particularly in the United Kingdom, due to thaumasite formation and replacement of the cement matrix.

Thaumasite is composed of charged $[Ca_3Si(OH)_6(H_2O)_{12}]^{4+}$ columns running parallel to the c-axis

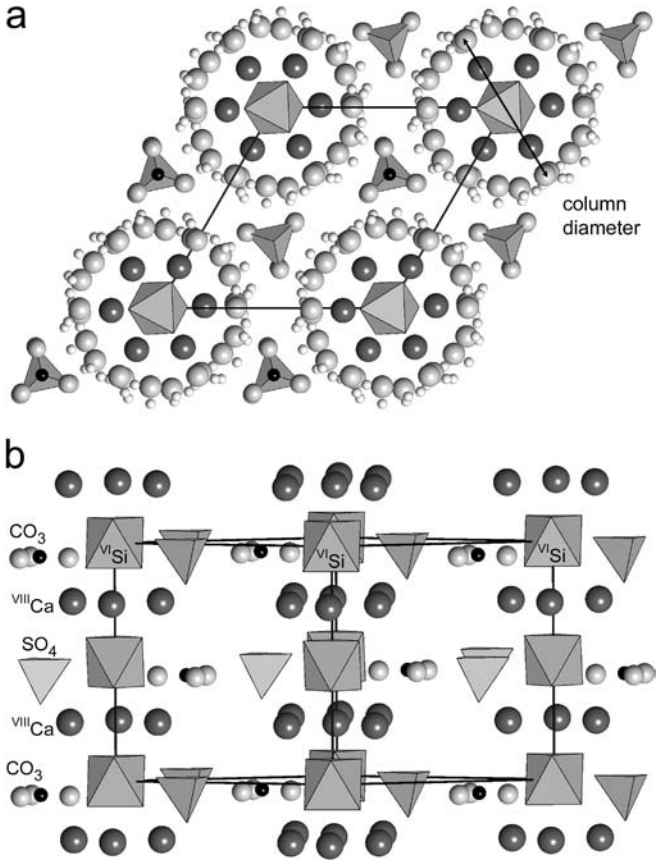

Fig. 1a, b Structure of thaumasite projected on (0001) (**a**) and (1120) (**b**). The hydrated silicate octahedron $[^{VI}Si(OH_6)]^{2-}$ and sulfate tetrahedron are shown as polyhedra. Carbon is represented by *small black spheres*, calcium by *large dark gray spheres*, oxygen by *intermediate light gray spheres*, and hydrogen by the *smallest white spheres*. The oxygen coordinated to Ca are water molecules that form the edge of the $[Ca_3Si(OH)_6(H_2O)_{12}]^{4+}$ columns, excluded in (**b**) for clarity. Expansivity of the column structures is dominated by lengthening of the *R*(Ca–O) and the *R*(O...O) hydrogen bonds on hydroxyl bonded to ^{VI}Si

(Fig. 1). Ca is coordinated to eight oxygens, four of which are molecular waters, and four hydroxyls. The result is a distorted tetragonal antiprism for Ca each sharing two edges with other Ca polyhedra. The columns are interconnected solely by hydrogen bonding with the $(SO_4)^{2-}$ and $(CO_3)^{2-}$ groups, which alternate along the *c*-axis and are fully ordered. Silicon sits on the axis of the columns and is six-coordinated by two crystallographically distinct hydroxyl $(OH)^-$ groups.

Thaumasite provides the opportunity to study fully hydrated, six-coordinate silicon within its stability field at room and low temperatures, and ambient pressure. In addition, recent studies show that thaumasite is a major phase associated with failure of Portland cement by sulfate attack, thus warranting a new investigation of this usual structure. Our main objective is to report details of structure refinements at 130 and 298 K as well as thermal expansion coefficients determined from cell parameters at 50-K intervals. The location of all ten H positions is achieved with reasonable precision at both 130 and 298 K, and will facilitate future ab initio calculations of hydrogen bonding geometry and interpretation of vibrational spectra of thaumasite and other hydrous minerals.

Experimental

A transparent single crystal of thaumasite measuring approximately $200 \times 150 \times 100$ μm was selected from fine-grained pure thaumasite bulk material from the University of Colorado mineral collection, but originating from an unknown locality. Microprobe analysis indicates that the material is essentially pure end-member thaumasite. Individual crystals were prechecked for quality by the X-ray precession method because many showed twinning or complex mosaic structure. The crystal showing the sharpest diffraction peak profiles was optically centered on a Siemens P4 four-circle diffractometer equipped with an 18-kW Mo-rotating anode generator operating at 50 kV and 250 mA. The instrument has an incident-beam graphite monochromator, and the effective wavelength ($K\alpha_1$ and $K\alpha_2$ mix ~0.71090 Å) is determined from cell refinement of a standard ruby crystal. The thaumasite cell dimensions were determined at room temperature from the centered positions of 20 independent low-angle reflections and found to be: $a = 11.0538(6)$ Å; $c = 10.4111(8)$ Å; with vol. = 1101.67(10) Å^3 (Table 1). Variable-speed θ–2θ scans ranging from 2° to 20° 2θ min^{-1} were used to measure 4703 reflection intensities (3238 unique) between 4°and 70°degrees 2θ in $P6_3$ with $+h$, $+k$, $\pm l$. The average $I/\sigma(I)$ for this dataset is 27.6. After data merging (Rint = 0.009), 2872 unique reflections with $I > 3\sigma(I)$ were corrected for Lorentz and polarization effects and used in the model refinement. An extinction parameter was refined, but is less than 0.0004. A 3σ cutoff was chosen because it provided us with the cleanest difference maps for hydrogen atom location without losing too many weak reflections.

Using initial atom positions from Effenberger et al. (1983), the structure model parameters were refined using SHELX-97 (Sheldrick 1997). For initial convergence, all ten hydrogen positions were held fixed. Next, all the hydrogen positions were allowed to vary using a fixed isotropic displacement parameter $U_{eq.} = 0.04$ (Å^2). The positions for H(12), H(19), H(25), H(35), H(45), and H(46) were stable, so the isotropic displacement parameter was allowed to refine, resulting in reasonable O–H distances. H(74), H(83), H(36), and the *x*/*a* parameter of H(26) were not stable, so the positions were chosen from the largest residuals in the difference-Fourier and held fixed during the final cycles of least-squares. The final model is fully converged with $R(F) = 0.028$, $wR(F) = 0.027$, and goodness of fit of 1.40.

Next, unit-cell parameters were measured using the same set of 20 independent reflections at temperatures 230, 180, and finally 130 K (Table 1). The four-circle diffractometer is equipped for low-temperature studies near liquid nitrogen temperatures with a flexible cryogenic gas nozzle; however, the amount of N_2 used for cooling below 130 K is excessive. Various temperatures are achieved through a heating device in the nozzle and calibrated using a Cu/Cu–Ni thermocouple (Yang and Smyth, 1996). The temperature can be held stable to within ±2° below 250 K. Cell parameters at 230, 180, and 130 K are listed in Table 1. Finally, 3912 intensity data were collected at 130 K in a fashion similar to

Table 1 Variation of thaumasite cell parameters with temperature

Temperature	130 K	180 K	230 K	298 K
a (Å)	11.022(2)	11.029(2)	11.037(2)	11.0538(6)
c (Å)	10.374(2)	10.383(2)	10.393(2)	10.4111(8)
Vol. (Å^3)	1091.4(2)	1093.68(16)	1096.49(17)	1101.67(10)
ρ_{calc} (g/cm^{-3})	1.894(1)	1.890(1)	1.885(1)	1.876(1)

Table 2 Structure of thaumasite (excluding hydrogen) with displacement parameters × 100 at 298 K (*first row*) and at 130 K (*second row*)

Atom	*x*/*a*	*y*/*b*	*z*/*c*	U_{11}	U_{22}	U_{33}	U_{12}	U_{13}	U_{23}	U_{eq}
Ca	0.19495(2)	0.98830(2)	0.25133[a]	1.184(9)	1.433(10)	1.097(8)	0.733(8)	−0.018(15)	0.019(15)	1.203(7)
	0.19400(4)	0.98719(4)	0.25133[a]	0.591(16)	0.699(16)	0.471(12)	0.346(13)	−0.031(25)	0.013(25)	0.576(12)
Si	0	0	0.00178(10)	0.962(12)	$=U_{11}$	0.744(18)	0.481(6)	0	0	0.889(10)
	0	0	0.00181(17)	0.52(2)	$=U_{11}$	0.27(3)	0.262(11)	0	0	0.440(18)
C	1/3	2/3	0.4623(3)	1.30(6)	$=U_{11}$	2.54(14)	0.65(3)	0	0	1.71(6)
	1/3	2/3	0.4603(4)	0.60(10)	$=U_{11}$	0.80(16)	0.30(5)	0	0	0.67(9)
S	1/3	2/3	0.98382(7)	1.157(15)	$=U_{11}$	1.83(3)	0.579(7)	0	0	1.382(13)
	1/3	2/3	0.98374(10)	0.53(3)	$=U_{11}$	0.81(4)	0.263(12)	0	0	0.62(2)
O(1)	0.39147(11)	0.22797(12)	0.2522(2)	1.67(5)	1.99(5)	4.70(7)	0.62(4)	−0.43(9)	−0.05(9)	2.92(4)
	0.39117(15)	0.22671(15)	0.2510(3)	0.71(7)	1.06(7)	2.09(7)	0.36(6)	−0.21(12)	−0.13(12)	1.32(5)
O(2)	0.26162(12)	0.40268(11)	0.2511(2)	2.66(5)	1.81(4)	2.41(5)	0.61(4)	0.54(8)	0.43(8)	2.52(4)
	0.26288(16)	0.40164(15)	0.2516(3)	1.23(7)	0.96(6)	0.91(6)	0.27(5)	0.17(11)	0.37(11)	1.12(5)
O(3)	0.00286(15)	0.33941(15)	0.07047(18)	1.93(7)	1.67(7)	3.15(8)	0.81(5)	−0.07(5)	0.89(5)	2.29(6)
	0.0044(2)	0.3391(2)	0.0695(2)	0.92(10)	0.67(10)	1.34(10)	0.35(8)	0.04(7)	0.36(8)	1.00(8)
O(4)	0.0246(2)	0.34872(18)	0.43169(17)	1.95(6)	2.00(7)	2.91(8)	0.87(5)	0.30(5)	−0.63(6)	2.33(6)
	0.0251(3)	0.3488(3)	0.4324(2)	0.84(9)	0.97(10)	1.21(10)	0.26(8)	0.09(7)	−0.32(8)	1.09(8)
O(5)	0.20088(17)	0.62300(18)	0.45809(16)	1.49(6)	2.30(7)	3.86(7)	0.91(6)	0.04(6)	−0.12(6)	2.57(6)
	0.2004(2)	0.6227(2)	0.45773(19)	0.65(9)	0.89(10)	1.50(8)	0.37(8)	0.02(7)	0.00(7)	1.02(7)
O(6)	0.19215(16)	0.62270(17)	0.03198(15)	1.52(6)	2.34(7)	3.14(6)	0.92(5)	0.50(6)	0.25(6)	2.36(5)
	0.1914(2)	0.6230(2)	0.03244(19)	0.76(9)	1.04(10)	1.24(8)	0.40(8)	0.28(8)	0.14(8)	1.04(8)
O(7)	0.13062(13)	0.12439(13)	0.10542(13)	1.08(5)	1.20(5)	0.94(6)	0.39(5)	−0.03(4)	−0.06(4)	1.16(4)
	0.1317(2)	0.1245(2)	0.1055(2)	0.64(9)	0.66(9)	0.31(10)	0.26(8)	0.07(7)	0.00(7)	0.57(8)
O(8)	0.13044(13)	0.12471(13)	0.39610(12)	1.14(6)	1.06(5)	1.12(6)	0.38(5)	0.07(4)	0.11(4)	1.18(5)
	0.1313(2)	0.1247(2)	0.3958(2)	0.38(9)	0.47(9)	0.67(10)	0.00(8)	0.04(7)	0.00(7)	0.61(8)
O(9)	1/3	2/3	0.84184(19)	2.61(7)	$=U_{11}$	1.82(9)	$=U_{11}/2$	0	0	2.34(5)
	1/3	2/3	0.8406(3)	1.22(9)	$=U_{11}$	0.63(11)	$=U_{11}/2$	0	0	1.03(7)

[a] *z*/*c* parameter of Ca is fixed to define the origin of the unit cell for comparison with Effenberger et al. (1983)

Table 3 Positional and displacement parameters (×100) of the hydrogen atoms in thaumasite at 298 K (*first row*) and at 130 K (*second row*)

atom	*x*/*a*	*y*/*b*	*z*/*c*	U_{eq}
H(74)	0.203[a]	0.179[a]	0.068[a]	0.030[a]
	0.204[a]	0.184[a]	0.064[a]	0.013[a]
H(83)	0.196[a]	0.195[a]	0.431[a]	0.030[a]
	0.194[a]	0.181[a]	0.436[a]	0.014[a]
H(12)	0.382(2)	0.291(3)	0.234(3)	0.042(7)
	0.371(3)	0.285(3)	0.248(5)	0.017(7)
H(19)	0.477(3)	0.270(3)	0.276(3)	0.055(8)
	0.472(3)	0.264(3)	0.267(4)	0.032(9)
H(25)	0.304(2)	0.465(3)	0.325(2)	0.021(6)
	0.318(4)	0.475(5)	0.330[a]	0.04(1)
H(26)	0.300[a]	0.441(3)	0.201(3)	0.057(12)
	0.287(4)	0.438(4)	0.200(3)	0.014(10)
H(35)	0.417(2)	0.076(2)	0.048(2)	0.017(5)
	0.409(4)	0.073(4)	0.044(3)	0.029(10)
H(36)	0.069[a]	0.422[a]	0.056[a]	0.030[a]
	0.062(4)	0.413(4)	0.054(3)	0.018[a]
H(45)	0.097(3)	0.451(3)	0.443(3)	0.046(8)
	0.099(4)	0.452(4)	0.442(4)	0.028(11)
H(46)	0.386(3)	0.032(3)	0.434(3)	0.024(7)
	0.389(5)	0.043(4)	0.439(4)	0.030[a]

[a] Parameter fixed during the final cycles of least-squares refinement

that at room temperature (with some restrictions due to the nozzle) resulting in 2634 unique reflections with 2333 having $I > 3\sigma(I)$. The structure was refined at 130 K using the room temperature model for starting positions. Final model atom positions for the nonhydrogen atoms are listed in Table 2 and for the hydrogen atoms in Table 3. The 130 K model is fully converged with $R(F) = 0.036$, $wR(F) = 0.029$, and a goodness of fit = 1.17.

Discussion

Unit-cell parameters of thaumasite at various temperatures are listed in Table 1, and plotted in Fig. 2. Expansion of the *a*- and *c*-axis directions is very similar, especially considering the major differences in structure parallel and perpendicular to the $[Ca_3Si(OH)_6 12(H_2O)]^{4+}$ columns. The mean coefficient of thermal expansion over the experimental temperature range from 130 to 300 K in the direction parallel to the columns is $\alpha_c = 2.1(2) \times 10^{-5}\ K^{-1}$, with $\alpha_a = 1.7(1) \times 10^{-5}\ K^{-1}$ in the direction between the columns. This is rather unusual considering that hydrogen bonding to the sulfate and carbonate groups is the dominant intracolumn support. Thermal expansion of thaumasite cell parameters is clearly nonlinear over this temperature range, but we have not fit data to a polynomial function because there are only three values (Table 4).

There are nine crystallographically unique oxygen sites in thaumasite, all of which participate in hydrogen bonding. Referring to Fig. 1, O(1) through O(4) are water molecules coordinated to calcium. O(5) is coordinated to carbon forming the carbonate group, and is hydrogen-bonded to O(2) through (O4). The sulfate tetrahedron has O(9) at its apex, hydrogen-bonded to O(1) of the column, and three O(6) basal oxygens hydrogen-bonded to O(2), O(3), and O(4). Finally, O(7) and O(8) are hydroxyl $(OH)^-$ groups and are coordinated to silicon and calcium. The hydrogen atom positions indicate in the first character the proton donor oxygen, and in the second the acceptor oxygen, so

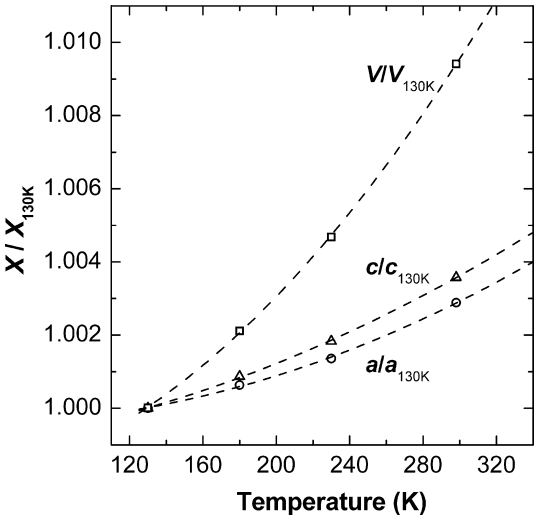

Fig. 2 Thermal expansion of thaumasite between 130 and 300 K

H(36), for example, forms the hydrogen bond O(3)–H(36)...O(6) between the column and the base of the sulfate tetrahedron. Bond distances, angles, and coordination polyhedra parameters for the structure at 130 and 298 K are listed in Table 5. The geometry of molecular water, the two hydroxyl groups, and all ten hydrogen bonds at 130 and 298 K are listed in Table 6.

None of the carbonate oxygens is hydroxyl or water. Edge and Taylor (1971) reported an exceptionally large deviation of the carbonate group from planarity of 0.15(3) Å, in the direction away from the apical oxygen O(9) of the sulfate tetrahedron. The refinements of Zemann and Zobetz (1981) and Effenberger et al. (1983) also found rather large deviations in carbonate planarity of 0.094(19) Å and 0.060(9) Å, respectively, but in the opposite direction — towards the apical oxygen of the sulfate tetrahedron. In our thaumasite structure, the carbonate group deviation from planarity is less than all previous refinements; 0.044(3) Å at 298 K and 0.026(5) Å at 130 K, again in the direction towards the apical oxygen of sulfate. These values are, in fact, not so unusual for carbonate minerals, where C typically lies ~0.02 Å above the oxygen plane (Reeder 1983). The carbonate group bond lengths are, however, rather large with R(C–O5) = 1.293(2) Å, exhibiting zero-thermal expansion between 130 K and room temperature. A survey of about 30 carbonate minerals shows that the average R(C–O) bond length is 1.284 Å, with 0.004 being the standard deviation in the mean (Zemann 1981). The longer C–O bonds in thaumasite are most likely the result of the rather strong hydrogen bonds on O(5), with R(O5...O4) = 2.675(2) Å, being by far the shortest hydrogen bond in the structure.

As with the carbonate groups, none of the sulfate group oxygens in hydroxyl or H_2O. The sulfate group in thaumasite shows significant negative thermal expansion between 130 and 298 K (Fig. 3). The three shorter S–O bonds with O(6) shorten from 1.477(2) Å at 130 K to 1.471(2) Å at room temperature. The longer S–O bond to the apical oxygen O(9) shows a somewhat smaller shortening from 1.482(3) Å at 130 K to 1.478(2) Å at room temperature. Granger and Protas (1969) reported some disorder between the carbonate and sulfate groups in the isostructural mineral jouravskite, $Ca_3[Mn(OH)_6](SO_4)(CO_3)\cdot 12H_2O$, but we find no evidence for positional or rotational disorder of the carbonate groups in the difference-Fourier, and observe only a small degree of anisotropy of the S, O(6), and O(9) displacement parameters.

The $[Ca_3Si(OH)_612(H_2O)]^{4+}$ columns in the thaumasite structure are largely bound together by the sulfate and carbonate groups via hydrogen bonding. O(1) through O(4) (molecular waters) form the outer wall of the column structures that runs parallel to the c-axis (Fig. 1), and their average position from the origin in the (0001) plane is used to estimate the column diameter D = 7.536(2) Å at 130 K and D = 7.569(2) Å at 298 K. This results in a mean coefficient of thermal expansion for the column diameter $\alpha_D = 2.6(2) \times 10^{-5}$ K^{-1}, which is ~1.5 times (or 8σ) greater than the mean thermal expansion between the columns (from the centroid at Si) given by $\alpha_a = 1.7(1) \times 10^{-5}$ K^{-1}.

The hydrated silicate octahedron in thaumasite shows zero or slightly negative thermal expansion between 130 and 300 K with $\alpha_V[^{VI}Si(OH)_6] = -0.6 \pm 1.1 \times 10^{-5}$ K^{-1} (Fig. 3). The $Si(OH)_6^{2-}$ group consists of three (equiva-

Table 4 Mean thermal expansion coefficients[a] ($\times 10^{-5}$ K^{-1}) for various components of thaumasite structure

Temperature range:	130–180 K	180–230 K	230–298 K	130–298 K
α_a	1.3 ± 0.7	1.5 ± 0.5	2.2 ± 0.2	1.7 ± 0.1
α_c	1.7 ± 0.7	1.9 ± 0.6	2.6 ± 0.2	2.1 ± 0.2
α_V	4.2 ± 0.7	5.1 ± 0.6	6.9 ± 0.4	5.6 ± 0.2
$\alpha_V(^{VIII}CaO_8)$				5.7 ± 1.0
$\alpha_V(^{VI}SiO_6)$				−0.6 ± 1.1
$\alpha_V(^{IV}SO_4)$				−5.8 ± 1.4
α_R(C–O)				0.0 ± 1.8
α_V(NPV)[b]				5.7 ± 1.2
$\alpha_R <$(O...O)$>_{hydroxyl}$[c]				4.7 ± 1.0
$\alpha_R <$(O...O)$>_{water}$[c]				2.4 ± 1.0
$[Ca_3Si(OH)_6(H_2O)_{12}]^{4+}$ column diameter				2.6 ± 0.2

[a] Mean thermal expansion coefficient is $(1/V_1)(V_2–V_1)/(T_2–T_1)$

[b] Nonpolyhedral volume

[c] Mean coefficient of thermal expansion for the average hydrogen bond distance involving hydroxyl or molecular water

Table 5 Variation of the coordination polyhedra in thaumasite with temperature

Bond	130 K	298 K
$[Ca(H_2O)_4(OH)_4]^{2-}$ polyhedron		
Ca–O(1)	2.440(1) Å	2.446(1) Å
Ca–O(2)	2.508(1)	2.518(1)
Ca–O(3)	2.414(2)	2.419(2)
Ca–O(4)	2.405(2)	2.406(2)
Ca–O(7a)	2.468(3)	2.479(2)
Ca–O(7d)	2.452(2)	2.461(1)
Ca–O(8b)	2.463(3)	2.476(2)
Ca–O(8d)	2.440(2)	2.450(1)
Average $R(^{VIII}Ca–O)$	2.449	2.457
Volume	25.97(3) Å^3	26.22(2) Å^3
$[Ca_3Si(OH)_6(H_2O)_{12}]^{4+}$ column diameter	7.536(2) Å	7.569(2) Å
$[Si(OH)_6]^{2-}$ octahedron		
Si–O(7) (×3)	1.777(2) Å	1.776(1) Å
Si–O(8) (×3)	1.790(2)	1.790(1)
Average $R(^{VI}Si–O)$	1.784	1.783
Volume	7.522(8) Å^3	7.515(4) Å^3
Angle variance[a]	12.3590	13.1460
Quad. elongation[a]	1.0034	1.0036
$<\Delta_{SiOH}>$[b]	0.0028 Å^2	0.0036 Å^2
$(SO_4)^{2-}$ tetrahedron		
S–O(6) (x3)	1.477(2) Å	1.471(2) Å
S–O(9)	1.482(3)	1.478(2)
Average $R(^{IV}S–O)$	1.478	1.473
Volume	1.656(2) Å^3	1.640(2) Å^3
Angle variance[a]	0.3510	0.2490
Quad. elongation[a]	1.0001	1.0001
$(CO_3)^{2-}$ group		
C–O(5) (×3)	1.293(2) Å	1.293(2) Å
elevation of C	0.026(2) Å	0.044(2) Å

[a] Polyhedral angle variance and quadratic elongation calculated by the method of Robinson et al. (1971) using XTALDRAW (see Downs and Heese 2001)
[b] Average difference in mean-squares displacement amplitude along the Si–OH vectors

Table 6 Variation of molecular water, hydroxyl, and hydrogen bonding in thaumasite with temperature

Atoms	130 K		298 K	
	Distance (Å)	Angle (°)	Distance (Å)	Angle (°)
Water molecules				
O1-H12	0.78(4)		0.78(3)	
O1-H19	0.79(3)		0.86(3)	
H12-O1-H19		107(3)		101(3)
O2-H25	1.10(2)		0.98(2)	
O2-H26	0.65(3)		0.67(3)	
H25-O2-H26		105(3)		104(3)
O3-H35	0.88(3)		0.91(2)	
O3-H36	0.76(3)		0.84(3)	
H35-O3-H36		105(5)		105(2)
O4-H45	1.02(3)		1.01(3)	
O4-H46	0.74(3)		0.65(2)	
H45-O4-H46		105(5)		99(3)
Hydroxyl groups				
O7-H74	0.85(3)		0.82(3)	
O8-H83	0.78(3)		0.84(3)	
Hydrogen bonds				
O1...O2	2.906(3)		2.926(2)	
H12...O2	2.14(4)		2.23(3)	
O1-H12...O2		166(3)		149(3)
O1...O9	2.811(2)		2.818(1)	
H19...O9	2.03(4)		1.97(3)	
O1-H19...O9		168(4)		169(3)
O2...O5	2.735(3)		2.748(2)	
H25...O5	1.65(3)		1.76(2)	
O2-H25...O5		172(3)		179(2)
O2...O6	2.796(3)		2.807(2)	
H26...O6	2.15(3)		2.16(3)	
O2-H26...O6		176(5)		166(3)
O3...O5	2.752(4)		2.748(3)	
H35...O5	1.91(4)		1.87(2)	
O3-H35...O5		162(5)		162(2)
O3...O6	2.781(3)		2.792(2)	
H36...O6	2.03(4)		1.96(3)	
O3-H36...O6		169(5)		169(2)
O4...O5	2.662(3)		2.675(2)	
H45...O5	1.65(4)		1.67(3)	
O4-H45...O5		172(5)		173(4)
O4...O6	2.759(4)		2.772(3)	
H46...O6	2.07(4)		2.17(2)	
O4-H46...O6		155(5)		154(3)
O7...O4	2.919(3)		2.939(2)	
H74...O4	2.08(4)		2.14(2)	
O7-H74...O4		168(5)		163(3)
O8...O3	2.924(3)		2.950(2)	
H83...O3	2.15(4)		2.14(2)	
O8-H83...O3		169(5)		163(3)

lent) longer bonds to O(8) and three shorter bonds to O(7), illustrated in Fig. 4 with thermal displacement ellipsoids enclosing 99.99% of the probability density. At room temperature, R(Si–O7) = 1.776(1) Å and R(Si-O8) = 1.790(1) Å. The average value, $\langle R(^{VI}Si–OH)\rangle = 1.783$ Å is about 10σ shorter than the average anhydrous six-coordinate Si–O bond in various anhydrous high-pressure silicates with $\langle R(^{VI}Si–O)\rangle = 1.794$ Å (Table 7). This is consistent with the fact that the Pauling bond strength sum around the hydroxyl oxygens bonded to the Si are all less than 2.0, indicating underbonding of these oxygens in thaumasite, whereas the silicate oxygen sites in the high-pressure anhydrous silicates are not underbonded.

Variation of the thaumasite structure with temperature between 130 and 298 K is listed in Table 5, and plotted in Fig. 3 as Lagrangian strain relative to the minimum temperature ($X/X_{130} - 1$) such that elements with positive thermal expansion have positive slope in Fig. 3. Although the unit cell, $^{VIII}CaO_8$ polyhedron, and nonpolyhedral volume show similar and significant positive thermal expansion over this temperature range, the silicate octahedron and sulfate tetrahedron show zero or negative volumetric thermal expansion, with $\alpha_V[^{VI}Si(OH)_6] = -0.6 \pm 1.1$ and $\alpha_V(^{IV}SO_4) = -5.8 \pm 1.4$ ($\times 10^{-5}$ K^{-1}). Most of the thermal expansion in the structure is accommodated by lengthening of all eight R(Ca–O) bonds and the R(O...O) hydrogen bond distances by on average 5σ, causing the $[Ca_3Si(OH)_6(H_2O)_{12}]^{4+}$ columns to both expand and move apart.

We have located with reasonable precision all ten hydrogen positions at both 130 and 298 K. At room temperature the average molecular water H–O–H angle

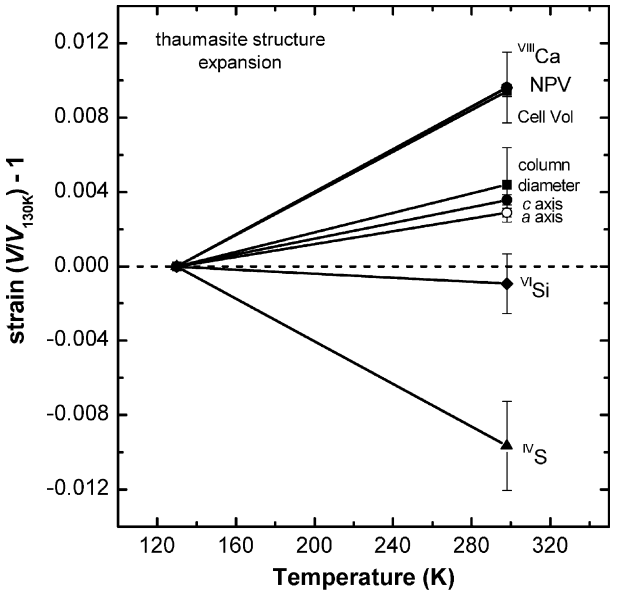

Fig. 3 Thermal expansion of the various components of the thaumasite structure between 130 and 300 K. Volume changes are plotted as Lagrangian strain relative to 130 K such that negative slope indicates a negative thermal expansion coefficient. The $[^{VI}Si(OH_6)]^{2-}$ octahedron exhibits zero or slightly negative thermal expansion; $\alpha(^{VI}Si) = -0.6 \pm 1.0 \times 10^{-5}$ K^{-1} over this temperature range

in thaumasite is 102.3°, with the average O–H distance $\langle R(O–H)\rangle = 0.84$ Å. At 130 K, the average molecular water angle is equal within uncertainty to the ideal (isolated) H_2O angle of 105°, with the average H–O–H angle being 105.5° and $\langle R(O–H)\ \rangle = 0.84$ Å.

At room temperature, the hydrogen bond distances, R(O...O), range from 2.675(2) Å for R(O4...O5) on the carbonate group, to 2.950(2) Å for R(O8...O3) on ^{VI}Si, with the mean hydrogen bond length at room temperature of 2.818 Å. The average hydrogen bond distance involving hydroxyl (bonded to silicon) is significantly larger than the average hydrogen bond distance involving hydroxyl, with $\langle R(O...O)\text{hydroxyl}\rangle = 2.945$ Å, and $\langle R(O...O)\text{water}\rangle = 2.786$ Å. At 130 K, the average hydrogen bond angle (O–H–O) in the structure is 168(4)°, being statistically equal to that found at room temperature, 165(3)°. However, the average hydrogen bond distance at 130 K is 2.805 Å, or about 7σ shorter. Furthermore, the two longer hydrogen bonds around the OH groups expand about twice as much (0.023 Å) as those around molecular water, with an average increase in R(O...O) of 0.011 Å. Therefore, while most of the thermal expansion in the structure is accommodated by increases in hydrogen bond distances, the hydrogen bond angles remain essentially invariant. The mean coefficient of thermal expansion for the hydrogen bonds are $\alpha = 2.4 \times 10^{-5}$ K^{-1} for those of molecular water (between the columns) and $\alpha = 4.7 \times 10^{-5}$ K^{-1} for the two on hydroxyl that are bonded to ^{VI}Si, which explains why the columns effectively expand (in diameter) more than they separate.

Finally, we calculated the electrostatic site potentials for all the oxygen positions in thaumasite using a simple nominal-valence point charge model (Smyth 1989). Excluding O7 and O8, oxygen site potentials range from about 30 to 35 V, being fairly typical values for carbonates (Smyth 1989). When hydrogen is not included (by modeling O7 and O8 as hydroxyls with −1 charge) the site potentials at O7 and O8 are extremely shallow, 15.2 and 15.0 V, respectively. Upon adding H to the model using our H74 and H83 positions, we calculate 27.8 and 27.5 V for O7 and O8, respectively. This relatively simple calculation confirms that the silicate-oxygen sites O7 and O8 in thaumasite would without the additional protons be drastically underbonded, facilitating this most unusual coordination of Si by $(OH)^-$ upon hydration.

Fig. 4 Details of the hydrated silicate octahedron in thaumasite at 298 and 130 K showing displacement ellipsoids enclosing 99.99% of the probability density. The R(Si–OH) bonds are relatively short, being essentially invariant over this temperature range, and shorter than most anhydrous ^{VI}Si–O bonds in high-pressure phases (Table 7). Without H, the O7 and O8 sites would have extremely shallow electrostatic potentials, given in the text

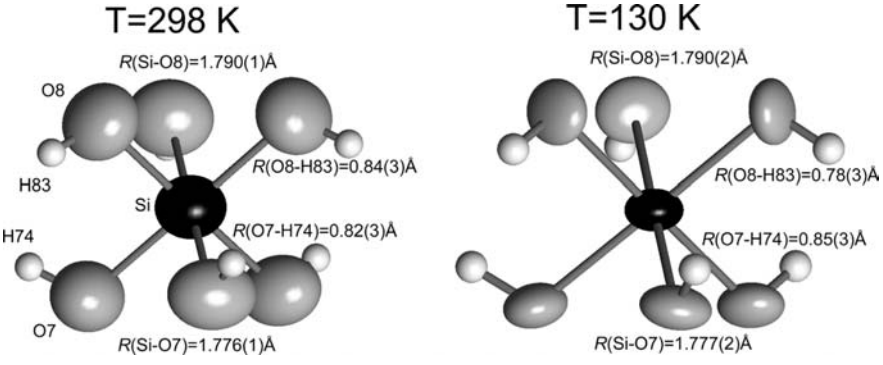

Conclusions

In summary, we have investigated thermal expansion of the thaumasite structure with refinements of the crystal structure at 130 and 298 K and measurement of the unit-cell parameters at several temperatures in this range. The new single-crystal thermal expansion data are the first of their kind for a structure containing silicon in six-coordination with hydroxyl. The immediate

Table 7 Crystal chemistry of hydrous and anhydrous six-coordinate silicon in minerals

	Thaumasite $Ca_3Si(OH)_6(CO_3)(SO_4)\cdot 12H_2O$	Phase D $MgSi_2H_2O_6$	Stishovite SiO_2	Ilmenite-$MgSiO_3$	Tetragonal majorite garnet-$MgSiO_3$	Orthorhombic silicate perovskite-$MgSiO_3$
$R(^{VI}Si–OH)$ Å	1.776(1) (×3) 1.790(1) (×3)	1.805 (×6)				
$R(^{VI}Si–O)$ Å			1.756 (×4) 1.813 (×2)	1.830 (×3) 1.768 (×3)	1.835 (×2)[a] 1.793 (×2)[a] 1.792 (×2)[a]	1.801 (×2) 1.796 (×2) 1.783 (×2)
$<R(^{VI}Si–OH)>$ Å	1.783	1.805				
$<R(^{VI}Si–O)>$ Å			1.775	1.799	1.807	1.793
Average octahedral edge length Å	2.520	2.554	2.508	2.541	2.555	2.536
Average octahedral angle	107.9	106.4	108.0	105.4	108.0	108.0
Octahedral volume $Å^3$	7.515	7.747	7.370	7.592	7.857	7.681
Octahedral angle variance	13.15	29.22	28.35	52.77	0.47	1.60
Mean octahedral Quadratic elongation	1.0036	1.0080	1.0084	1.0152	1.0004	1.0005
Reference	Current study	Yang et al. (1997)	Ross et al. (1990)	Horiuchi et al. (1982)	Angel et al. (1989)	Horiuchi et al. (1987)

[a] Modeled as $(Si_{0.8}Mg_{0.2})$ at this site

coordination polyhedra around the tetravalent and hexavalent cations C, Si, and S all show zero or negative thermal expansion, whereas the CaO_8 polyhedron and the interpolyhedral hydrogen bond distances all show large positive thermal expansions. Thermal expansion of the two R(O...O) hydrogen bond distances on the hydroxyl groups, O7 and O8 bonded to ^{VI}Si, is on average twice as great as those coordinated to water, on O1 through O4 coordinated to ^{VIII}Ca atoms. The result is that although the column structures running parallel to c are largely held together by hydrogen bonding to the sulfate and carbonate groups, the columns expand more than they move apart over this temperature range. This explains why the structure is not stable to very high temperature; the onset of dehydration is observed only at 383 K (Brough and Atkinson 2001).

The silicate hydroxyl octahedron in thaumasite shows zero or slightly negative thermal expansion over the experimental temperature range. The octahedron is composed of two symmetrically unique, relatively short Si–OH bonds with $\langle R(^{VI}Si–OH)\ \rangle = 1.783$ Å, being roughly 0.01 Å (or 10σ) shorter than the average $R(^{VI}Si–O)$ for the high-pressure phases containing ^{VI}Si, listed in Table 7. This is rather unusual considering that for known structures containing Si in tetrahedral coordination with hydroxyl, the average $R(^{IV}Si–OH)$ bond is on average 0.02 Å longer than $R(^{IV}Si–O)$. Calculation of electrostatic site potentials for the oxygen positions in thaumasite confirms that without H, the silicon in thaumasite would be significantly underbonded.

Acknowledgements This work was supported by the National Science Foundation through grant EAR 97-25672 to J. Smyth. S. Jacobsen wishes to acknowledge support from the Alexander von Humboldt Foundation and the Bayerisches Geoinstitut during preparation of the manuscript. We thank Hexiong Yang for assistance with the experiments and John Sharp for insightful discussion about thaumasite.

References

Angel RJ, Finger LW, Hazen RM, Kanzaki M, Weidner DJ, Liebermann RC, Veblen DR (1989) Structure and twinning of single-crystal $MgSiO_3$ garnet synthesized at 17 GPa and 1800° C. Am Mineral 74: 509–512

Aguilera J, Blanco Varela MT, Vázquez (2001) Procedure of sythesis of thaumasite. Cement Concrete Res 31: 1163–1168

Barnett SJ, Adam CD, Jackson ARW (2000) Solid solutions between ettringite, $Ca_6Al_2(SO_4)_3(OH)_{12}\cdot 26H_2O$, and thaumasite, $Ca_3SiSO_4CO_3(OH)_6\cdot 12H_2O$. J Mat Sci 35: 4109–4114

Bensted J (1999) Thaumasite – background and nature in deterioration of cements, mortars and concretes. Cement Concrete Composites 21: 117–121

Bickley JA (1999) The repair of Arctic structures damaged by thaumasite. Cement Concrete Composites 21: 155–158

Brough AR, Atkinson A (2001) Micro-Raman spectroscopy of thaumasite. Cement Concrete Res 31: 421–424

Crammond NJ (1985) Thaumasite in failed cement mortars and renders from exposed brickwork. Cement Concrete Res 15: 1039–1050

Downs RT, Hesse PJ (2001) Animation of crystal structure variations with pressure, temperature and composition. In: Hazen RM, Downs RT (eds) High-temperature and high-pressure crystal chemistry. Rev Mineral Geochem 41: 89–117

Downs RT, Gibbs GV, Bartelmehs KL, Boisen MB (1992) Variations of bond lengths and volumes of silicate tetrahedra with temperature. Am Mineral 77: 751–757

Edge RA, Taylor HFW (1969) Crystal structure of thaumasite, a mineral containing $[Si(OH)_6]^{2-}$ groups. Nature 224: 363–364

Edge RA, Taylor HFW (1971) Crystal structure of thaumasite, $[Ca_3Si(OH)_6{\cdot}12H_2O]$ $(SO_4)(CO_3)$. Acta Crystallogr (B) 27: 594–601

Effenberger H, Kirfel A, Will G, Zobetz E (1983) A further refinement of the crystal structure of thaumasite, $Ca_3Si(OH)_6CO_3SO_412H_2O$. N Jb Miner Mh 2: 60–68

Finger LW, Hazen RM (2001) Systematics of high-pressure silicate structures. In: Hazen RM, Downs RT (eds) High-temperature and high-pressure crystal chemistry. Reviews in Mineralogy and Geochemistry 41: 123–155

Frost DJ, Fei Y (1998) Stability of phase D at high pressure and high temperature. J Geophys Res 103: 7463–7474

Gibbs GV (1982) Molecules as models for bonding in silicates. Am Mineral 67: 421–450

Granger MM, Protas J (1969) Détermination et étude de la structure crystalline de la jouravskite $Ca_3Mn^{IV}(SO^4)(CO_3)(OH)_6{\cdot}12H_2O$. Acta Crystallogr (B) 25: 1943–1951

Grimmer AR, Wieker W, Lampe F, Fechner E, Peter R, Molgedey G (1980) Hochauflösende ^{29}Si-NMR an festen silicaten: Anisotropie der chemischen Verschiebung im thaumasite. Z Chem 20: 453

Hartshorn SA, Sharp JH, Swamy RN (1999) Thaumasite formation in Portland limestone cement pastes. Cement Concrete Res 29: 1331–1340

Hazen RM, Downs RT, Prewitt CT (2001) Principles of comparative crystal chemistry. In: Hazen RM, Downs RT (eds) High-temperature and high-pressure crystal chemistry. Reviews in Mineralogy and Geochemistry 41: 1–33

Hobbs DW, Taylor MG (2000) Nature of the thaumasite sulfate attack mechanism in field concrete. Cement Concrete Res 30: 529–533

Horiuchi H, Hirano M, Ito E, Matsui Y (1982) $MgSiO_3$ (ilmenite-type): single-crystal X-ray diffraction study. Am Mineral 67: 788–793

Horiuchi H, Ito E, Weidner DJ (1987) Perovskite-type $MgSiO_3$: single-crystal X-ray diffraction study. Am Mineral 72: 357–360

Jacobsen SD, Smyth JR, Swope RJ, Sheldon RI (2000) Two proton positions in the very strong hydrogen bond of serandite, $NaMn_2[Si_3O_8(OH)]$. Am Mineral 85: 745–752

McDonald AM, Peterson OV, Gault RA, Johnsen O, Niedermayr G, Branstätter F (2001) Micheelsenite, $(Ca, Y)_3Al(PO_3OH, CO_3)(CO_3)(OH)_6 \cdot 12H_2O$, a new mineral from Mont Saint-Hilaire, Quebec, Canada and the Nanna pegmatite, Narsaarsuup Qaava, South Greenland. Neues Jahrbuch für Mineralogie Monatshefte 8: 337–351

Moenke H (1964) Ein weiteres Mineral mit Silizium in 6er-Koordination: Thaumasit. Naturwissenschaften 51: 239

Moore A, Taylor HFW (1970) Crystal structure of ettringite. Acta Crystallogr (B) 26: 386–393

Nyfeler D, Armbruster T (1998) Silanol groups in minerals and inorganic compounds. Am Mineral 83: 119–125

Pauling L (1980) The nature of silicon–oxygen bonds. Am Mineral 65: 321–323

Prewitt CT, Downs RT (1998) High-pressure crystal chemistry. In: Hemley RJ (ed) Ultrahigh-pressure mineralogy. Reviews in Mineralogy, vol 37, Mineralogical society of America, 284–317

Reeder RJ (1983) Crystal chemistry of the rhombohedral carbonates. In: Reeder RJ (ed) Carbonates: mineralogy and chemistry. Reviews in Mineralogy, vol 11, Mineralogical society of America, 1–47

Ross NL, Shu JF, Hazen RM (1990) High-pressure crystal chemistry of stishovite. Am Mineral 75: 739–747

Robinson K, Gibbs GV, Ribbe PH (1971) Quadratic elongation: a quantitative measure of distortion in coordination polyhedra. Science 172: 567–570

Santhanam M, Cohen MD, Olek J (2001) Sulfate attack research – wither now? Cement Concrete Res 31: 845–851

Sheldrick GM (1997) SHELX-97, Program for crystal structure refinement. University of Göttingen, Gemany

Smyth JR (1989) Electrostatic characterization of oxygen sites in minerals. Geochem Cosmochim Acta 53: 1101–1110

Smyth JR, Jacobsen SD, Hazen RM (2001) Comparative crystal chemistry of orthosilicate minerals. In: Hazen RM, Downs RT (eds) High-temperature and high-pressure crystal chemistry. Reviews in Mineralogy and Geochemistry 41: 187–209

Stebbins JF, Kanzaki M (1991) Local structure and chemical shifts for six-coordinated silicon in high-pressure mantle phases. Science 251: 294–298

Yang H, Prewitt CT, Frost DJ (1997) Crystal structure of the dense hydrous magnesium silicate, phase D. Am Mineral 82: 651–654

Yang H, Smyth JR (1996) Crystal structure of a $P2_1/m$ ferromagnesian cummingtonite at 140 K. Am Mineral 81: 363–368

Zemann J (1981) Zur Stereochemie der Karbonate. Fortschr Miner 59: 95–116

Zemann J, Zobetz E (1981) Do the carbonate groups in thaumasite have anomalously large deviations from coplanarity? Kristallografija 26: 1215–1217